

Published in final edited form as:

*Biochemistry*. 2013 February 26; 52(8): 1437–1445. doi:10.1021/bi301442x.

## The oxidation mode of pyranose 2-oxidase is controlled by pH

Methinee Prongjit<sup>‡</sup>, Jeerus Sucharitakul<sup>§</sup>, Bruce A. Palfey<sup>§</sup>, and Pimchai Chaiyen<sup>‡,\*</sup>

<sup>‡</sup>Department of Biochemistry and Center of Excellence in Protein Structure and Function, Faculty of Science, Mahidol University, Bangkok, 10400, Thailand <sup>§</sup>Department of Biochemistry, Faculty of Dentistry, Chulalongkorn University, Henri-Dunant Road, Patumwan, Bangkok, 10300, Thailand <sup>§</sup>Department of Biological Chemistry, University of Michigan Medical School, 1150 W. Medical Center Dr., Ann Arbor, MI 48109-5606, USA

### Abstract

Pyranose 2-oxidase (P2O) from *Trametes multicolor* is a flavoenzyme that catalyzes the oxidation of D-glucose and other aldopyranose sugars at the C2 position by using O<sub>2</sub> as an electron acceptor to form the corresponding 2-keto-sugars and H<sub>2</sub>O<sub>2</sub>. In this study, the effects of pH on the oxidative half-reaction of P2O were investigated using stopped-flow spectrophotometry. The results showed that flavin oxidation occurred via different pathways depending on the pH of the environment. At pH values lower than 8.0, reduced P2O reacts with O<sub>2</sub> to form a C4a-hydroperoxy-flavin intermediate, leading to elimination of H<sub>2</sub>O<sub>2</sub>. At pH 8.0 and higher, the majority of the reduced P2O reacts with O<sub>2</sub> via a pathway which does not allow detection of the C4a-hydroperoxy-flavin, and flavin oxidation occurs with decreased rate constants upon the rise in pH. The switching between the two modes of P2O oxidation is controlled by protonation of a group which has a pK<sub>a</sub> of 7.6 ± 0.1. Oxidation reactions of reduced P2O under rapid pH change as performed by stopped-flow mixing were different from the same reactions performed with enzyme pre-equilibrated at the same specified pH values, implying that the protonation of the group which controls the mode of flavin oxidation cannot be rapidly equilibrated with outside solvent. Using a double-mixing stopped-flow experiment, a rate constant for proton dissociation from the reaction site was determined to be 21.0 ± 0.4 s<sup>-1</sup>.

### Keywords

pyranose oxidase; C4a-hydroperoxy-flavin; flavoprotein oxidase; oxidative half-reaction; transient kinetics; pH effects

Pyranose 2-oxidase (P2O) from *Trametes multicolor* is a flavoenzyme that catalyzes the oxidation of D-glucose and other aldopyranose sugars at the C2 position using O<sub>2</sub> as an electron acceptor. Products of the reaction are the corresponding 2-keto-sugars and H<sub>2</sub>O<sub>2</sub> (Scheme 1)<sup>1,2</sup>. As the reaction of P2O can generate H<sub>2</sub>O<sub>2</sub>, an essential substrate for lignin degrading enzymes such as lignin peroxidase and manganese peroxidase, P2O is thought to have an important role in lignocellulose degradation.<sup>1</sup> The enzyme has also been proposed to be used in biofuel cell applications.<sup>3</sup> Sequence analysis and crystal structures of P2O indicate that the enzyme belongs to the glucose-methanol-choline (GMC) oxidoreductase superfamily of flavoproteins.<sup>4,5</sup> This enzyme is a homotetrameric protein which contains one FAD molecule per subunit that is covalently linked via a methyl group of FAD at the

\*To whom correspondence should be addressed: Pimchai Chaiyen, Department of Biochemistry and Center for Excellence in Protein Structure and Function, Faculty of Science, Mahidol University, Rama 6 Road, Bangkok, 10400, Thailand. Tel. 662-201-5596; Fax 662-354-7174; pimchai.cha@mahidol.ac.th.

C8-position to the N<sup>3</sup> of His167.<sup>5,6</sup> In general, the reaction of P2O can be divided into a reductive half-reaction in which the FAD cofactor is reduced by a sugar substrate and an oxidative half-reaction where the reduced enzyme reacts with oxygen to form oxidized FAD and H<sub>2</sub>O<sub>2</sub>.<sup>2,7</sup> The role of the FAD covalent linkage is to increase the enzyme's oxidative power for the reductive half-reaction.<sup>8</sup> The crystal structure of P2O (1.8 Å) in complex with acetate, a competitive inhibitor of the enzyme, shows a closed conformation in which the substrate loop (residues 452-457) closes off the active site from outside solvent.<sup>5</sup> The crystal structure of His<sub>6</sub>-P2O-His167Ala in complex with the more slowly oxidized substrate, 2-fluoro-2-deoxy-D-glucose, shows an open conformation in which the substrate loop swings out to provide space to accommodate the sugar ligand.<sup>9</sup> Recently, another enzyme conformation in which the substrate loop swings half-way between the open and closed conformation was crystallized in complex with 3-fluoro-3-deoxyglucose.<sup>10</sup> This substrate loop was proposed to be a dynamic loop which can swing out when the sugar binds during the reductive half-reaction and swing in to close off the active site from solvent during the oxidative half-reaction.<sup>10,11</sup>

The reaction mechanism of P2O from *T. multicolor* has been investigated at pH 7.0 using steady-state and pre-steady state kinetics, site-directed mutagenesis and kinetic isotope effects.<sup>2,7,8,12-14</sup> Wild-type P2O catalyzes the reaction using a Ping-Pong mechanism at pH 7.0.<sup>2</sup> In a mutant P2O in which Thr169 is mutated to an Ala residue, the hydrogen bond between residue 169 and the N5 atom of FAD is absent, resulting in a change in the kinetic mechanism to one that consists of a ternary complex.<sup>12</sup> Steady-state kinetic studies of P2O from *T. ochracea* have demonstrated a change in the P2O kinetic mechanism from a Ping-Pong type mechanism at pH values below 7.0 to a ternary complex type mechanism at pH values above 7.0.<sup>15</sup> The switching of reaction mechanism from the Ping-Pong to the ternary complex type may be resulting from the change of structural dynamics of the substrate loop in the T169A mutant or at higher pH values. Investigation of the reductive half-reaction of wild-type P2O using D-glucose and 2-*d*-D-glucose at pH 7.0 indicated that D-glucose binds to the enzyme through a 2-step binding process; the first step is the initial complex (E-Fl<sub>ox</sub>:G\*) formation while the second step is an isomerization to form an active Michaelis complex (E-Fl<sub>ox</sub>:G).<sup>2</sup> Mutation of Thr169 to an Ala residue results in a 1600-fold decrease in the  $k_{red}$ , suggesting that the interaction between Thr169 and FAD is important for the reduction of the flavin.<sup>12</sup> The covalent-linkage between His167 and C8 $\alpha$  of FAD is important for flavin reduction, as the H167A mutant showed a 22-fold decrease in  $k_{red}$  when compared to that of the wild-type P2O.<sup>8</sup> Studies of solvent isotope effects on the transient kinetics of wild-type P2O and the H167A mutant showed no solvent isotope effect on any of the steps during the reductive half-reaction.<sup>8</sup> Recent investigation on the reductive half-reaction of WT enzyme and H548 mutants at various pH values have shown that His548 exists in a deprotonated form in the resting state of the oxidized enzyme, and this residue serves as the catalytic base that abstracts a proton at the C2-OH of D-glucose to generate an alkoxide intermediate prior to the hydride transfer step.<sup>14</sup>

Investigation into the oxidative half-reaction of P2O at pH 7.0 has shown that the reduced enzyme reacts with O<sub>2</sub> to form a C4a-hydroperoxy-flavin intermediate.<sup>7</sup> The enzyme is so far the only one in the flavoprotein oxidase class in which C4a-hydroperoxy-flavin can be detected under natural turnover conditions.<sup>7</sup> Besides the C4a-adduct found in P2O, the intermediate was also detected in the crystal structure of choline oxidase.<sup>16</sup> C4a-hydroperoxy-flavin forms during the oxidative half-reaction of the H167A mutant with similar rate constants as the wild-type enzyme, implying that the covalent linkage is not an important factor for the formation of C4a-hydroperoxy-flavin.<sup>8</sup> In contrast, precise positioning and orientation of Thr169 in relation to the flavin N5/O4 locus is required for stabilization of the C4a-hydroperoxy-flavin, as mutation of Thr169 to other residues (Ser, Asn, Ala, and Gly) fails to stabilize C4a-hydroperoxy-flavin during the oxidative half-

reaction of P2O.<sup>12</sup> Recently, investigations on the mechanism of H<sub>2</sub>O<sub>2</sub> elimination from the C4a-hydroperoxy-flavin in the wild-type P2O using kinetic isotope effects and transient kinetics have revealed that the breakage of the flavin N5-H bond controls the overall process of H<sub>2</sub>O<sub>2</sub> elimination from the C4a-hydroperoxy-flavin.<sup>13</sup> From a mechanistic point of view, P2O is an ideal model for exploring the factors required for the formation of C4a-hydroperoxy-flavin in a flavoenzyme because this enzyme has served as the missing link between flavoprotein monooxygenases in which formation of C4a-(hydro)peroxy-flavin is common and flavoprotein oxidases in which the C4a-(hydro)peroxy-flavin is absent.<sup>7,17,18</sup>

In this study, the effects of pH on the oxidative half-reaction of P2O have been investigated using stopped-flow spectrophotometry. The results showed that flavin oxidation occurred via different pathways at lower and higher pH values. Different mixing experiments indicate that a group with a pK<sub>a</sub> of ~7.7 must be present in its protonated state for the formation of a detectable C4a-hydroperoxy-flavin intermediate.

## Materials and Methods

### Reagents

D-Glucose, all buffers (MES, Gly-Gly, CHES, and CAPS), cytochrome c, superoxide dismutase, and xanthine oxidase were purchased from Sigma-Aldrich Company. Xanthine was purchased from Nutritional Biochemical Corporation. Spin-labeled reagent 5-(diethoxyphosphoryl)-5-methyl-1-pyrroline-N-oxide (DEPMPO) was purchased from Alexis<sup>®</sup> Biochemicals. P2O concentrations were calculated based on the extinction coefficient of an FAD bound per enzyme subunit,  $1.13 \times 10^4 \text{ M}^{-1}\text{cm}^{-1}$ .<sup>2</sup>

### Rapid reaction experiments

Reactions were carried out in 50 mM buffer at 4 °C. Buffers used for maintaining pH were MES for pH 5.5, sodium phosphate for pH 6-7.5, Gly-Gly for pH 8-8.5, CHES for pH 9.0 and CAPS for pH 9.5-11.0. Rapid kinetics were performed using a stopped-flow spectrophotometer, TgK Scientific models SF-62DX or SF-61DX in single-mixing or double-mixing modes with a 1 cm optical path-length of the observation cell. The stopped-flow apparatus was made anaerobic by flushing the flow system with an anaerobic buffer solution containing protocatechuate/protocatechuate dioxygenase as previously described.<sup>7</sup> A solution of reduced enzyme was prepared by titrating oxidized enzyme with a solution of 10 mM D-glucose in the same buffer in an anaerobic glove-box (Belle Technology). The reduced enzyme solution was put into a tonometer and then loaded onto the stopped-flow machine. Buffers (5 mM) containing various oxygen concentrations were prepared using air-saturation or bubbling buffers for 8 min with a 50% O<sub>2</sub>/N<sub>2</sub> gas mixture, 100% oxygen, and 100% oxygen on ice. This produced buffers containing 0.13 mM, 0.31 mM, 0.61 mM, and 0.96 mM oxygen, respectively (concentrations after stopped-flow mixing). Reactions were monitored at various wavelengths using a photomultiplier tube or a photo diode-array detector. Apparent rate constants ( $k_{\text{obs}}$ ) from kinetic traces using a photomultiplier tube as a detector were calculated from exponential fits using software Kinetic studio RC5 (TgK Scientific, Bradford-on-Avon, UK) or Program A (developed by R. Chang, C-J. Chiu, J. Dinverno and D.P. Ballou, at University of Michigan, Ann Arbor, USA). Determinations of microscopic rate constants associated with the upper pathway in Scheme 2 were carried out by plotting  $k_{\text{obs}}$  versus oxygen concentrations and analyzing with Marquardt-Levenberg nonlinear fit algorithms implemented in KaleidaGraph (Synergy Software, Reading, PA) and Equations 1-2 described below.

## Results

### Oxidation of the reduced P2O at various pH values

Anaerobic solutions of the reduced enzyme (20  $\mu\text{M}$ , final concentration after stopped-flow mixing) that had been equilibrated in 50 mM of the various buffers at different pH values (Materials and Methods) were mixed with the same buffers containing various oxygen concentrations using a stopped-flow spectrophotometer. This process was repeated at several pH values over the range of pH 5.5–10.0 and the results are shown in Figure 1. Previous reports of P2O kinetics at pH 7.0 have shown that this reaction is biphasic and can be explained by a two-step consecutive model (upper path of Scheme 2).<sup>2,7</sup> The first phase consists of formation of C4a-hydroperoxy-flavin ( $k_1$ ), which typically displays an increase in absorbance at 395 nm and a lag phase at 458 nm. The second phase is elimination of  $\text{H}_2\text{O}_2$  from C4a-hydroperoxy-flavin ( $k_2$ ) to give oxidized enzyme, which shows a decrease in absorbance at 395 and a large increase in absorbance at 458 nm.<sup>2,7</sup> At pH 7.0, rate constants associated with Scheme 2 (upper pathway) can be analyzed according to Equations 1-2 using graphical and kinetic simulation methods. Details for the analysis are described elsewhere.<sup>7</sup>

$$k_{obs1} = k_1[O_2] + k_{-1} + k_2 - \frac{k_1 k_2 [O_2]}{k_1 [O_2] + k_{-1} + k_2} \quad (1)$$

$$k_{obs2} = \frac{k_1 k_2 [O_2]}{k_1 [O_2] + k_{-1} + k_2} \quad (2)$$

The kinetics of reduced P2O reacting with oxygen at various pH values monitored at 395 nm and 458 nm showed two phases (Figure 1). The first phase is reflected by an absorbance increase at 395 nm and a small change in the absorbance at 458 nm. The absorbance increase at 395 nm in this phase was largest at the lowest pH investigated (5.5, Figure 1A). When the pH was increased, the amplitude of the absorbance at 395 nm during the first phase decreased and appeared to be only a lag phase at pH 9.5 and 10.0 (Figure 1B). The  $k_{obs}$  values of this phase ( $k_{obs1}$ ) were rather constant between pH 5.5 and 7.5, with slopes of the plots of  $k_{obs1}$  versus the oxygen concentration of  $7.5 \pm 0.8 \times 10^4 \text{ M}^{-1} \text{ s}^{-1}$  at pH 5.5 and  $6.7 \pm 0.5 \times 10^4 \text{ M}^{-1} \text{ s}^{-1}$  at pH 7.5 (Table 1, Figure 2A). At pH 8.0, the apparent rate constant of the first phase decreased significantly to  $2.3 \pm 0.8 \times 10^4 \text{ M}^{-1} \text{ s}^{-1}$  (Table 1, Figure 1A), and the absorbance signal change appeared as a lag phase. The absorbance change was not significant enough for analysis at pH 8.5 - 10.0 (Figure 1B).

The second kinetic phase was characterized by a decrease in absorbance at 395 nm and a large increase in absorbance at 458 nm (Figure 1C). Observed rate constants of this phase were rather constant over the pH range of 5.5 – 7.5 with limiting rate constants of  $28 \pm 5 \text{ s}^{-1}$  at pH 5.5 and  $21 \pm 2 \text{ s}^{-1}$  at pH 7.5 (Table 1, Figure 2B). However, at pH 8.0 and higher, the  $k_{obs}$  of the second phase decreased significantly and appeared to be lower at higher pH values (Table 1, Figure 2B). The saturation rate constant at pH 10.0 was  $1.3 \pm 0.3 \text{ s}^{-1}$  (Table 1, Figure 2C). A plot of the saturation rate constants of the second phase, the elimination of  $\text{H}_2\text{O}_2$  from C4a-hydroperoxy-flavin, versus pH revealed a decreasing trend for the rate constants with a rise in pH (Table 1, Figure 3A) with a calculated  $p_a$  of  $7.8 \pm 0.1$ . Thus, the data suggest that the mechanism of  $\text{H}_2\text{O}_2$  generation to form the oxidized enzyme is different between the reactions at lower and higher pH values. At pH 8.0 and higher, P2O was oxidized via a mechanism which generated  $\text{H}_2\text{O}_2$  to form oxidized enzyme significantly slower than the mechanism at lower pH values (Figure 1B-C, Scheme 2).

## Investigation on absorption characteristics of the intermediate during oxidation of reduced P2O at pH 10.0

The results from Figures 1-3 imply that the oxidation mechanisms of reduced P2O at higher and lower pH values are different. At pH values higher than 8.5, the first phase of reduced P2O oxidation appeared to be a lag in absorbance at both 395 and 458 nm (Figure 1). In order to identify the absorption characteristics of the intermediate resulting from the first phase at high pHs, an experiment similar to those shown in Figure 1 was performed, and the absorption changes at all wavelengths were monitored at pH 10.0 using stopped-flow spectrophotometry (Materials and Methods). A solution of the reduced enzyme (27  $\mu\text{M}$ ) was mixed with a buffer containing 0.96 mM oxygen (final concentrations after mixing). The reaction was performed in 100 mM Gly-Gly buffer pH 10 at 4 °C using a stopped-flow spectrophotometer. The wavelengths for detection were varied at intervals of 5 nm over the range of 320-550 nm for single wavelength detection and the same experiment using diode-array detection was also carried out. Neither detection method indicated any significant absorption changes at any of the wavelengths after the initial lag phase was completed (data not shown), indicating that the oxidation of P2O at pH 10.0 does not occur via a pathway which stabilizes the formation of C4a-hydroperoxy-flavin. The rate constant associated with the initial lag phase could not be estimated accurately due to the absence of significant absorbance changes. A plot of the  $k_{\text{obs}}$  of the flavin oxidation phase at various oxygen concentrations yielded a saturation value of  $1.3 \pm 0.3 \text{ s}^{-1}$  (Figure 2C). The hyperbolic dependence of  $k_{\text{obs}}$  on the oxygen concentration suggests that at least one more step preceding flavin oxidation exists (lower path in Scheme 2). The results indicate that the oxidation mechanism of P2O occurs via a pathway that stabilizes C4a-hydroperoxy-flavin at lower pH values and via a pathway in which no detectable C4a-adduct intermediate is found at higher pH values. Therefore, a plot of the absorbance increases at the end of the first phase at 395 nm (due to the formation of C4a-hydroperoxy-flavin, Figure 1A-B) versus the pH (Figure 3B) should allow determination of the  $\text{p}K_{\text{a}}$  of a group in the active site that controls the switching of the mechanism of flavin oxidation between the pathways observed at low and high pH values (Scheme 2). Protonation of this group is required for the oxidation of P2O to occur via the mechanism that supports C4a-hydroperoxy-flavin formation (Figure 3A and 3B). The plot in Figure 3B indicated a  $\text{p}K_{\text{a}}$  of  $7.6 \pm 0.1$ . A scheme depicting the kinetic mechanism of P2O oxidations at various pH values is summarized in Scheme 2. At higher pHs, because the  $k_{\text{obs}}$  of flavin oxidation reaches a limit, we propose that the first step of the reaction is the binding of  $\text{O}_2$  to P2O to form a binary complex of  $\text{E}_{\text{red}}:\text{O}_2^*$ . Due to the low proton concentrations in the outside solvent, formation of the intermediate at the second step occurs very slowly while the third step of the intermediate decay to form oxidized flavin occurs faster. This condition generally prevents kinetic detection of any intermediate. The current data cannot determine if the intermediate at higher pH is C4a-hydroperoxyflavin or other species.

## Reaction of the reduced P2O with oxygen at various pH values performed by pH-jump experiments

In order to address whether the group in the active site which controls the P2O oxidation mechanism (Scheme 2) can be rapidly equilibrated with outside solvent, experiments in which the pH of the reaction was rapidly changed upon stopped-flow mixing were carried out. A solution of the reduced P2O (40  $\mu\text{M}$ , before mixing) in 5 mM sodium phosphate pH 7.0 containing 100 mM sodium sulfate was mixed with 100 mM buffers of various pH values (Materials and Methods) containing various oxygen concentrations in order to obtain final pH values of 5.5, 6.6, 7.0, 7.5, 8.0, 8.5, 9.0, 9.5, 10.0, 10.5, and 11.0. The reactions were monitored at 395 nm and 458 nm (Figure 4). The results indicated that oxidations of reduced P2O under an abrupt change in pH upon stopped-flow mixing were different from the oxidations of the same enzymes pre-equilibrated at the same specified pH values (Figure

1). These data imply that the protonation of the group in the active site that controls the mode of flavin oxidation may be shielded and cannot be rapidly equilibrated with outside solvent. Kinetic traces of the pH-jump experiments at higher pH values such as those at pH 10.0 and 11.0 (Figure 4A) showed an absorption increase at 395 nm during the first phase, which indicated formation of C4a-hydroperoxy-flavin. These data indicate that upon stopped-flow mixing, proton dissociation from the group that controls the mode of flavin oxidation was incomplete even when the outside surrounding medium was at pH 10.0 or 11.0.

In the pH range of 5.5-8.0, the reaction in Figure 4 was biphasic with the first phase (0.002-0.02 s) having an absorbance increase at 395 nm and a lag at 458 nm, and the second phase (0.02-0.3 s) having an absorbance decrease at 395 nm and a large absorbance increase at 458 nm. Qualitatively, the kinetics of the reactions looked similar to those of the enzyme pre-equilibrated at the same final pH values (Figure 1A), particularly for reactions at pH 7.0 and lower. At pH 7.5 and 8.0, the experiments carried out by the pH-jump method (Figure 4A) showed a larger absorbance increase at 395 nm than the kinetic traces at the same pH in Figure 1. These results suggest that due to the slow dissociation of H<sup>+</sup> from the group that controls the oxidation mode, pH-jump mixing permits retention of the protonation state during this short time period, allowing a considerable amount of C4a-hydroperoxy-flavin to form at pH 7.5 and 8.0 in a manner described by the upper pathway in Scheme 2. At pH 9.0 – 11.0, the reaction was triphasic. The first phase consisted of an absorbance increase at 395 nm and a very small change at 458 nm, the second phase consisted of an absorbance decrease at 395 nm and an absorbance increase at 458 nm, and the third phase (0.3-10 s) consisted of an absorbance increase at both 395 and 458 nm (Figure 4A-B). Therefore, the second and third phases represented flavin oxidation via the upper and lower pathways in Scheme 2, respectively. The second phase was flavin oxidation via formation of the C4a-hydroperoxy-flavin, while the third phase was oxidation via the pathway that did not allow detection of any intermediate (lower pathway in Scheme 2). Upon increasing the pH, the lowering of the outside proton concentration shifted the state of the enzyme towards the unprotonated form that oxidized via the lower pathway in Scheme 2. Therefore, more of the flavin oxidation (larger A<sub>458</sub> increase) occurred at the third phase (Figure 4B). The data in Figure 4 suggest that the protonation state at the active site, which is not highly exposed to outside solvent, is a major factor that determines the mechanism of flavin oxidation.

### **A double-mixing stopped-flow experiment to measure the rate constant of proton dissociation from P2O**

A solution of 96  $\mu$ M reduced P2O in 5 mM MES pH 5.5 containing 100 mM sodium sulfate was mixed with an anaerobic solution of 100 mM CHES pH 9.0 during the first mixing step, and the reaction was delayed for various incubation times before a second mixing step took place with 0.96 mM oxygen in 100 mM CHES pH 9.0. The final solution (pH 9.0) contained 24  $\mu$ M reduced P2O and 0.48 mM oxygen. The reaction was monitored at 395 nm and 458 nm. The reaction showed three phases for short age-time mixings (when the enzyme was not fully equilibrated) but was reduced to two phases when the mixing age time was longer than 0.2 s (full equilibration reached) (Figure 5). The data were consistent with our previous results in which three phases were observed for oxidation of the enzyme upon mixing by the pH-jump method (Figure 4) and two phases were observed when the enzyme was pre-equilibrated at pH 9.0 (Figure 1B). Therefore, a plot of the absorbance changes at 395 nm during the first phase versus incubation time represents a time-dependent change of the enzyme from a partially to a fully equilibrated form at pH 9.0 (Inset of Figure 5A). The plot can be fit with an apparent rate constant of  $21.0 \pm 0.4 \text{ s}^{-1}$ , which corresponds to the rate constant of proton dissociation from the active site to give the unprotonated enzyme at pH 9.0 (Scheme 2).

## Oxidation of reduced P2O as performed by pH jumping from pH 9.0 to various pH values

A solution of the reduced enzyme (58  $\mu\text{M}$ ) in 5 mM CHES buffer pH 9.0 containing 100 mM sodium sulfate was mixed with buffers at various pH values at concentrations of 100 mM, including MES (pH 5.0 and 6.0), sodium phosphate (pH 7.0), or Gly-Gly (pH 8.0) containing 1.82 mM oxygen. The final solutions contained 29  $\mu\text{M}$  enzyme and 0.96 mM oxygen at pH values given in Figure 6. Kinetic traces of the reactions monitored at 395 nm (Figure 6) were biphasic, similar to those observed from the experiments where the enzyme was pre-equilibrated at the same final pH (overlaid data from Figure 1). However, the values of the observed rate constants for the formation and decay of the intermediate, and for the amplitude changes at 395 nm were less than those obtained when the experiment was performed with the pre-equilibrated enzyme (Figure 1). In agreement with the data in Figures 4-5, the results indicate incomplete equilibration of the internal protonation site prior to oxygen binding upon the quick pH change during stopped-flow mixing. The enzyme retained some kinetic characteristics of the reduced P2O at pH 9.0, thus resulting in slower rate constants and smaller amplitude changes in comparison to the data obtained in Figure 1 for the oxidation of P2O pre-equilibrated at pH 5.0, 6.0, and 7.0.

## Discussion

Our work herein demonstrated that at low and high pH values, reduced P2O reacts differently with oxygen and that the protonation state of P2O is a major factor in determining the mode of flavin oxidation (Scheme 2). Reduced P2O at pH values lower than 8.0 reacts with  $\text{O}_2$  to form a C4a-hydroperoxy-flavin intermediate, which has an absorption peak at 375 nm (Figure 1), before elimination of  $\text{H}_2\text{O}_2$  occurs with a rate constant of  $21 \pm 2 \text{ s}^{-1}$  at pH 7.5 (Table 1). At pH values of 8.5 and higher, the majority of the reduced P2O reacts with  $\text{O}_2$  via a pathway which does not allow detection of the C4a-hydroperoxy-flavin, and oxidation of the flavin occurs with lower rate constants as the pH is increased (Table 1, Figure 1-2). The switching between the two modes of P2O oxidation is controlled by the protonation of a group that has a  $p_a$  of  $7.6 \pm 0.1$  (Figure 3).

Oxidation of reduced P2O at lower pH values occurs through the formation of C4a-hydroperoxy-FAD. Protonation of a group in the active site is a key factor in promoting flavin oxidation via this pathway (Scheme 2). The current model for the reaction of reduced flavin with oxygen involves an initial single electron transfer from reduced flavin to  $\text{O}_2$  to form a radical pair between the flavin semiquinone and the superoxide radical (Scheme 3).<sup>18</sup> For flavoenzymes that do not stabilize C4a-hydroperoxyflavin such as Glucose 1-oxidase, this step has a high activation energy and is the rate-limiting step for the overall process of reduced flavin oxidation.<sup>19-21</sup> The flavin semiquinone:superoxide radical pair is not stable and has never been detected in the reactions of flavoprotein oxidases. In a recent study of glycolate oxidase, a flavin semiquinone species was detected during the enzyme oxidative half-reaction in  $\text{D}_2\text{O}$  at pD 5.<sup>22</sup> For P2O reactions, we could not detect any free superoxide based on EPR measurements and the flavin semiquinone could not be detected based on transient kinetic measurements (data not shown). P2O is different from most flavoprotein oxidases in that in the second step of the reaction, the radical pair collapses to generate a C4a-peroxy-FAD intermediate which is protonated rapidly at lower pHs to form C4a-hydroperoxy-FAD (Scheme 3).<sup>7,8,13</sup> A recent investigation on the P2O reaction mechanism using solvent kinetic isotope effects (SKIE) has shown that there is no significant SKIE for the formation of C4a-hydroperoxy-FAD at pH 7.0, indicating that the protonation process to generate C4a-hydroperoxy-FAD is rapid.<sup>13</sup> According to the active site structure of P2O<sup>9</sup> and the results of a recent study on the P2O reductive half-reaction<sup>14</sup>, His548 has the potential to be the residue that acts as a proton donor and an internal proton source to facilitate formation of C4a-hydroperoxy-FAD (Scheme 3). Our data in Figure 3 indicate that the protonation site that is required to be protonated in order to facilitate P2O oxidation via

the upper pathway in Scheme 2 has a  $pK_a$  value of  $7.6 \pm 0.1$ , which is a probable  $pK_a$  value for histidine.

Results from studies of the reductive half-reaction of P2O indicate that His548 likely exists in the protonated form at the initial stage of the oxidative half-reaction. For the reductive half-reaction, His548, which originally is in the unprotonated form, acts as a general base to abstract a hydroxyl proton from the C2-OH of D-glucose in order to facilitate formation of a D-glucose alkoxide intermediate.<sup>8,14</sup> A hydride equivalent is then transferred from the D-glucose alkoxide intermediate to the oxidized flavin to generate the reduced flavin and the 2-keto-D-glucose. According to this model, His548 should possess an extra proton after completing the reductive half-reaction. The protonated His548 may thus facilitate oxidation of the flavin via the upper pathway in Scheme 2 and may be an internal proton source which donates a proton to generate the C4a-hydroperoxy-flavin intermediate (Scheme 3). The following step of  $H_2O_2$  elimination is controlled by the breakage of the flavin N5-proton bond at pH 7.0 to form a hydrogen peroxide leaving group.<sup>13</sup> Thus, formation of C4a-hydroperoxy-FAD instead of C4a-peroxy-FAD would ensure the efficient generation of a  $H_2O_2$  product at lower pH values. According to the upper pathway in Scheme 2, upon finishing the reaction, His548 is deprotonated (Scheme 3), which is the form that is ready for catalyzing another catalytic cycle of P2O.

Detection of C4a-hydroperoxy-flavin by transient kinetics at lower pH values is also due to the slower rate of intermediate decay as compared to the faster rate of intermediate formation. At pH 7.0 and 0.96 mM oxygen, the  $k_{obs}$  of C4a-hydroperoxy-FAD formation is  $58 \text{ s}^{-1}$  while the  $k_{obs}$  of the following step of  $H_2O_2$  elimination from the intermediate is  $16 \text{ s}^{-1}$ .<sup>7</sup> Our recent investigation of P2O at pH 7.0 using transient kinetics and kinetic isotope effects has shown that the breakage of the flavin N5-H bond is the key step that controls the overall  $H_2O_2$  elimination process.<sup>13</sup> Studies of factors affecting the stability of C4a-hydroperoxy-flavin in the monooxygenase component ( $C_2$ ) of *p*-hydroxyphenylacetate hydroxylase, an enzyme which stabilizes a long-lived C4a-hydroperoxy-flavin, have shown that  $H_2O_2$  elimination is faster at higher pHs due to facilitation of the breakage of the flavin N5-H bond by the increase in hydroxide ion concentration.<sup>23-25</sup> The experiments in Figure 4, in which some C4a-hydroperoxy-FAD formation was retained at higher pH values due to incomplete equilibration of the enzyme, also showed that the  $H_2O_2$  elimination process (second phase) was slightly faster at higher pH (Figure 4A).

Oxidation of P2O pre-equilibrated at higher pH did not allow detection of a C4a-adduct intermediate, suggesting that the mechanism of reduced P2O oxidation is different from the reaction at lower pH values. At pH 10.0, at which the group that controls the mode of oxidation should be completely unprotonated, no intermediate with C4a-adduct characteristics was detected. The data only indicated a lag phase at all wavelengths investigated (data not shown) and flavin oxidation in the second phase was hyperbolically dependent on the oxygen concentrations (Figure 2C). The rate constant for the formation of intermediate at high pH was also much smaller than that for the reaction at lower pH. It is possible that the flavin oxidation at higher pH values occurs via an outer sphere  $O_2$  reduction, similar to reactions of other flavoprotein oxidases in which formation of C4a-hydroperoxy-flavin does not occur.

Overall, the oxidation of P2O occurs at a slower rate upon an increase in pH (Figure 1 and Table 1), which is similar to many reactions catalyzed by other flavoprotein oxidases such as D-amino acid oxidase,<sup>26</sup> choline oxidase,<sup>27</sup> monomeric sarcosine oxidase,<sup>28,29</sup> and aryl alcohol oxidase.<sup>30</sup> Studies of these enzymes suggest that a positive charge at the reaction site is required for efficient flavin oxidation. Studies by Klinman et al. have shown that protonation of His516 in glucose oxidase (GO) facilitates formation of a flavin



semiquinone:superoxide radical pair which is the rate-limiting step for the overall flavin oxidation process in GO.<sup>21,31,32</sup> We propose that at higher pH, the reaction site in P2O (His548) is in the unprotonated form which cannot efficiently facilitate the first electron transfer from reduced flavin to oxygen to form the flavin semiquinone radical pair or cannot donate a proton to generate the C4a-hydroperoxy-flavin intermediate as in the upper pathway of Scheme 2. Under these conditions, the proton can only be derived from the protons found in the outside solvent, the concentration of which is decreased at higher pHs. Therefore, flavin oxidation occurs at slower rates at higher pH values.

Results from figures 4-6 indicate that the proton equilibration process at the active site of P2O is not rapid and is incomplete during stopped-flow mixing, resulting in the observed differences between the kinetics obtained from pH-jump experiments and those obtained from reactions of enzymes pre-equilibrated at the same specified pH values. The double-mixing experiment in figure 5 indicates a rate constant for proton dissociation from the reaction site of  $21.0 \pm 0.4 \text{ s}^{-1}$ . A previous study has also shown that the rate of proton exchange for reduced P2O at the flavin N5-H is rather slow (less than  $2.3 \times 10^{-3} \text{ s}^{-1}$ ).<sup>13</sup> All of these data suggest that the environment at the P2O active site is quite enclosed. The equilibration process at the P2O active site may be limited by the movement of the substrate loop which can assume different conformations for reductive and oxidative half-reactions.<sup>9,11,33</sup>

In conclusion, our work has shown that the oxidative half-reaction of P2O occurs faster at lower pH than at higher pH. Formation of C4a-hydroperoxyflavin was detected at lower pH. The major factor that contributes to the formation of the intermediate and the efficient generation of H<sub>2</sub>O<sub>2</sub> at lower pH is the protonation of an active site group with a pK<sub>a</sub> of 7.6. The results presented herein are useful for understanding the nature of the P2O reaction and the factors facilitating formation of C4a-hydroperoxyflavin in flavoenzymes in general.

## Acknowledgments

This work was supported by The Thailand Research Fund through grants No. BRG5480001 (to P.C.), No. RSA5580050 (to J.S.), and No. PHD/0151/2547 from the Royal Golden Jubilee Ph.D. program (to M.P). B.A.P. was supported by a grant from NIH GM61087. Grants from the Faculty of Science, Mahidol University (to P.C.), and from the Faculty of Dentistry Chulalongkorn University (to J.S.) are also acknowledged.

## References

1. Leitner C, Volc J, Haltrich D. Purification and characterization of pyranose oxidase from the white rot fungus *Trametes multicolor*. *Appl Environ Microbiol.* 2001; 67:3636–3644. [PubMed: 11472941]
2. Prongjit M, Sucharitakul J, Wongnate T, Haltrich D, Chaiyen P. Kinetic mechanism of pyranose 2-oxidase from *Trametes multicolor*. *Biochemistry.* 2009; 48:4170–4180. [PubMed: 19317444]
3. Spadiut O, Pisanelli I, Maischberger T, Peterbauer C, Gorton L, Chaiyen P, Haltrich D. Engineering of pyranose 2-oxidase: improvement for biofuel cell and food applications through semi-rational protein design. *J Biotechnol.* 2009; 139:250–257. [PubMed: 19095017]
4. Albrecht M, Lengauer T. Pyranose oxidase identified as a member of the GMC oxidoreductase family. *Bioinformatics.* 2003; 19:1216–1220. [PubMed: 12835264]
5. Hallberg BM, Leitner C, Haltrich D, Divne C. Crystal structure of the 270 kDa homotetrameric lignin-degrading enzyme pyranose 2-oxidase. *J Mol Bio.* 2004; 341:781–796. [PubMed: 15288786]
6. Halada P, Leitner C, Sedmera P, Haltrich D, Volc J. Identification of the covalent flavin adenine dinucleotide-binding region in pyranose 2-oxidase from *Trametes multicolor*. *Anal Biochem.* 2003; 314:235–242. [PubMed: 12654310]

7. Sucharitakul J, Prongjit M, Haltrich D, Chaiyen P. Detection of a C4a hydroperoxyflavin intermediate in the reaction of a flavoprotein oxidase. *Biochemistry*. 2008; 47:8485–8490. [PubMed: 18652479]
8. Sucharitakul J, Wongnate T, Chaiyen P. Kinetic isotope effects on the noncovalent flavin mutant protein of pyranose 2-oxidase reveal insights into the flavin reduction mechanism. *Biochemistry*. 2010; 49:3753–3765. [PubMed: 20359206]
9. Kujawa M, Ebner H, Leitner C, Hallberg BM, Prongjit M, Sucharitakul J, Ludwig R, Rudsander U, Peterbauer C, Chaiyen P, Haltrich D, Divne C. Structural basis for substrate binding and regioselective oxidation of monosaccharides at C3 by pyranose 2-oxidase. *J Biol Chem*. 2006; 281:35104–35115. [PubMed: 16984920]
10. Tan TC, Haltrich D, Divne C. Regioselective control of  $\beta$ -d-glucose oxidation by pyranose 2-oxidase is intimately coupled to conformational degeneracy. *J Mol Biol*. 2011; 409:588–600. [PubMed: 21515286]
11. Spadiut O, Tan T, Pisanelli I, Haltrich D, Divne C. Importance of the gating segment in the substrate-recognition loop of pyranose 2-oxidase. *FEBS J*. 2010; 277:2892–2909. [PubMed: 20528921]
12. Pitsawong W, Sucharitakul J, Prongjit M, Tan T, Spadiut O, Haltrich D, Divne C, Chaiyen P. A Conserved Active-site Threonine Is Important for Both Sugar and Flavin Oxidations of Pyranose 2-Oxidase. *J Biol Chem*. 2010; 285:9697–9705. [PubMed: 20089849]
13. Sucharitakul J, Wongnate T, Chaiyen P. Hydrogen peroxide elimination from C4a-hydroperoxy-flavin in a flavoprotein oxidase occurs through a single proton transfer from flavin N5 to a peroxide leaving group. *J Biol Chem*. 2011; 286:16900–16999. [PubMed: 21454569]
14. Wongnate T, Sucharitakul J, Chaiyen P. Identification of a catalytic base for sugar oxidation in the pyranose 2-oxidase reaction. *Chembiochem*. 2011; 12:2577–2586. [PubMed: 22012709]
15. Rungsririyachai K, Gadda G. A pH switch effects the steady-state kinetic mechanism of pyranose 2-oxidase from *Trametes ocharcea*. *Arch Biochem Biophys*. 2009; 483:10–15.
16. Orville AM, Lountos GT, Finnegan S, Gadda G, Prabhakar R. Crystallographic, spectroscopic, and computational analysis of a flavin C4a-oxygen adduct in choline oxidase. *Biochemistry*. 2009; 48:720–728. [PubMed: 19133805]
17. Palfey BA, McDonald C. Control of catalysis in flavin-dependent monooxygenase. *Arch Biochem Biophys*. 2010; 493:26–36.
18. Chaiyen P, Fraaije MW, Mattevi A. The enigmatic reaction of flavins with oxygen. *Trends Biochem Sci*. 2012; 37:373–380. [PubMed: 22819837]
19. Bruice T. Oxygen flavin chemistry. *Israel J Chem*. 1984; 24:54–61.
20. Klinman J. Life as aerobes: are there simple rules for activation of dioxygen by enzyme? *J Bio Inorg Chem*. 2001; 6:1–13. [PubMed: 11191216]
21. Klinman J. How do enzymes activate oxygen without inactivating themselves? *Acc Chem Res*. 2007; 40:325–333. [PubMed: 17474709]
22. Pennati A, Gadda G. Stabilization of an intermediate in the oxidative half-reaction of human liver glycolate oxidase. *Biochemistry*. 2011; 50:1–3. [PubMed: 21141873]
23. Ruangchan N, Tongsook C, Sucharitakul J, Chaiyen P. pH dependent studies reveal an efficient hydroxylation mechanism of the oxygenase component of p-hydroxyphenyl acetate 3-hydroxylase. *J Biol Chem*. 2011; 286:223–233. [PubMed: 21030590]
24. Thotsaporn K, Chenprakhon P, Sucharitakul J, Mattavi A, Chaiyen P. Stabilization of C4a-hydroperoxy-flavin in a two-component flavin-dependent monooxygenase is achieved through interactions at flavin N5 and C4a atom. *J Biol Chem*. 2011; 286:28170–28180. [PubMed: 21680741]
25. Tongsook C, Sucharitakul J, Thotsaporn K, Chaiyen P. Interactions with the substrate phenolic group are essential for hydroxylation by the oxygenase component of p-hydroxyphenylacetate 3-hydroxylase. *J Biol Chem*. 2011; 286:44491–44502. [PubMed: 22052902]
26. Denu JM, Fitzpatrick PF. pH and kinetic isotope effect on the oxidative half-reaction of l-amino-acid oxidase. *J Biol Chem*. 1994; 269:15054–15059. [PubMed: 7910822]
27. Ghanem M, Gadda G. Effect of reversing the protein positive charge in the proximity of the flavin N(1) Locus of choline oxidase. *Biochemistry*. 45:3437–3447. [PubMed: 16519539]

28. Jorns MS, Chen Z, Mathews FS. Structure characterization of mutation at the oxygen activation site Monomeric sarcosine oxidase. *Biochemistry*. 2010; 49:3631–3639. [PubMed: 20353187]
29. Zhao G, Bruckner RC, Jorns MS. Identification of the oxygen activation site in monomeric sarcosine oxidase: role of Lys265 in catalysis. *Biochemistry*. 2008; 47:9124–9135. [PubMed: 18693755]
30. Hernandez-Ortega A, Lucas F, Ferreira P, Medina M, Gualla V, Martinez AT. Role of active site histidines in the two half-reactions of the aryl-alcohol oxidase catalytic cycle. *Biochemistry*. 2012; 51:6595–6608. [PubMed: 22834786]
31. Su Q, Klinman JP. Nature of oxygen activation in glucose oxidase from *Aspergillus niger*: the importance of electrostatic stabilization in superoxide formation. *Biochemistry*. 1999; 38:8572–8581. [PubMed: 10387105]
32. Roth JP, Klinman JP. Catalysis of electron transfer during activation of O<sub>2</sub> by the flavoprotein glucose oxidase. *Proc Natl Acad Sci USA*. 2003; 100:62–67. [PubMed: 12506204]
33. Tan T, Pitsawong W, Wongnate T, Spadiut O, Haltrich D, Chaiyen P, Divne C. H-bonding and positive charge at the N(5)/O(4) locus are crucial for covalent flavin attachment in *Trametes* pyranose 2-oxidase. *J Mol Bio*. 2010; 402:578–594. [PubMed: 20708626]
34. Chaiyen P. Flavoenzymes catalyzing oxidative aromatic ring-cleavage reactions. *Arch Biochem Biophys*. 2010; 493:62–70. [PubMed: 19728986]

## Abbreviations

<b>P2O</b>	pyranose 2-oxidase
<b>FAD</b>	flavin adenine dinucleotide
<b><i>k</i><sub>obs</sub></b>	observed rate constant
<b>GMC</b>	glucose-methanol-choline family
<b>E-Fl<sub>ox</sub></b>	P2O in the oxidized form
<b>E-Fl<sub>red</sub></b>	P2O in the reduced form
<b>EH-Fl<sub>red</sub></b>	the protonated form of reduced P2O
<b>E-Fl-OOH</b>	C4a-hydroperoxyflavin
<b>E-Fl-OO<sup>•</sup></b>	C4a-peroxyflavin

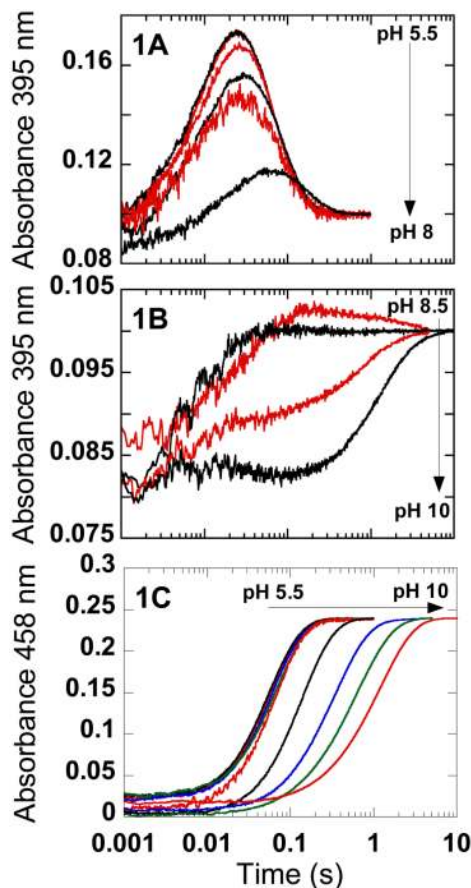


**Figure 1.**

Oxidation of reduced P2O at various pH values. Solutions of reduced P2O (20  $\mu$ M) pre-equilibrated in buffers at different pH values were mixed with the same buffers containing oxygen (0.96 mM) at 4  $^{\circ}$ C. Concentrations are given as final concentrations after mixing. (A) The kinetic traces show the increase (first kinetic phase) and decrease (second kinetic phase) of absorbance at 395 nm at pH 5.5 (red), 6.0 (black), 6.5 (red), 7.0 (black), 7.5 (red), and 8.0 (black). (B) The traces monitored at 395 nm for reactions at pH 8.5 (red), 9.0 (black), 9.5 (red), and 10.0 (black) do not show any large increase in absorbance at 395 nm as in (A). (C) The kinetic traces monitored at 458 nm show re-oxidation of the flavin at pH 5.5, 6.0, 6.5, 7.0 (superimposed), 7.5 (red), 8.0 (black), 8.5 (blue), 9.5 (green), and 10.0 (red). Arrows indicate the changes of kinetic traces according to pH increment.

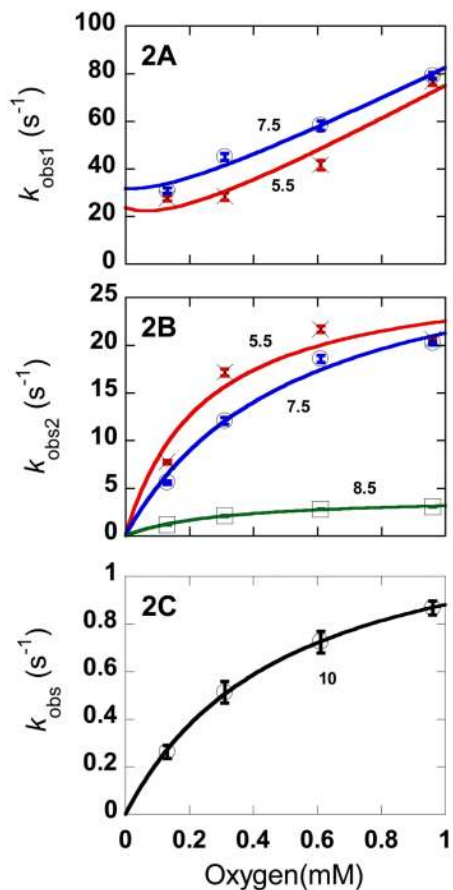


**Figure 2.**

Effects of pH on the kinetics of the oxidative half-reaction of P2O for the enzyme pre-equilibrated at various pH values. Observed rate constants from Figure 1 were plotted against oxygen concentration. (A) A plot of the observed rate constants of the first phase ( $k_{obs1}$ ) (the formation of intermediate) *versus* oxygen concentration at pH 5.5 and pH 7.5. (B) A plot of the observed rate constants of the second phase ( $k_{obs2}$ ), flavin reoxidation, *versus* oxygen concentration at low pH (pH 5.5 and 7.5) and high pH (pH 8.5). (C) A plot of the observed rate constants of the flavin reoxidation ( $k_{obs}$ ) *versus* the oxygen concentration at pH 10. It should be noted that reactions of reduced flavin and oxygen in most flavin-dependent monooxygenases are bimolecular with no intercept value (17, 23-25, 34). The intercept of P2O reaction in a low pH range may reflect the reversibility of C4a-hydroperoxyflavin formation that is different from flavin-dependent monooxygenases (8, 13).

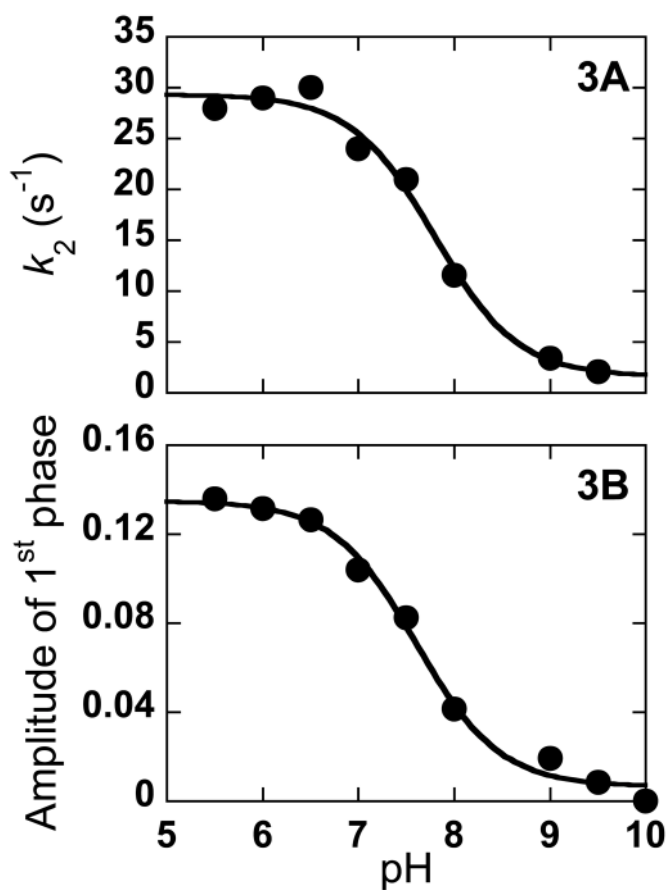


**Figure 3.** pH-Dependence of flavin oxidation. (A) A plot of the observed rate constants of the second phase from Figure 1 *versus* pH corresponds to a  $pK_a$  value of  $7.8 \pm 0.1$  (B) A plot of the amplitude changes of the first phase *versus* pH corresponds to a  $pK_a$  value of  $7.6 \pm 0.1$ .

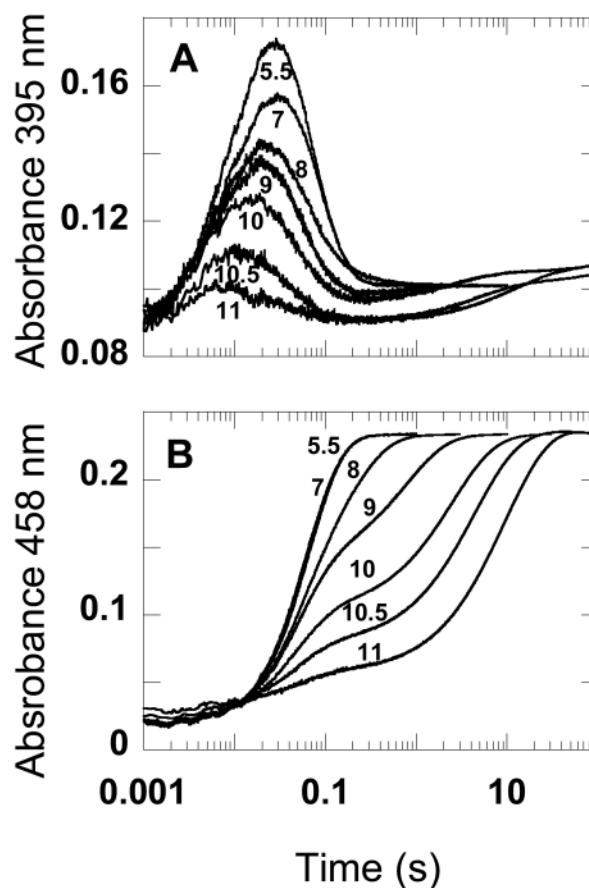


**Figure 4.** Kinetic traces of reduced P2O reacting with oxygen at various pH values performed by pH-jump mixings at 4 °C. A solution of reduced P2O (40  $\mu$ M) pre-equilibrated in 5 mM sodium phosphate and 100 mM sodium sulfate at pH 7.0 was mixed with buffers at pH 5.5-11 using the stopped-flow apparatus. Final solutions contained 20  $\mu$ M reduced enzyme and 0.96 mM oxygen in buffers at various pH values as indicated in the figures. (A) Absorbance change at 395 nm indicates formation and decay of a C4a-hydroperoxyflavin intermediate. (B) Absorbance change at 458 nm indicates flavin reoxidation.

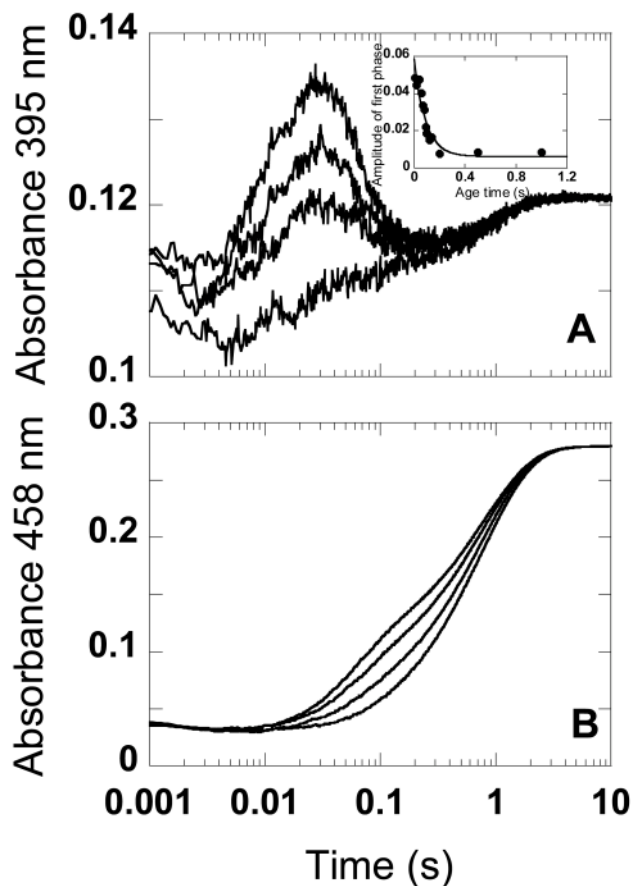


**Figure 5.** Double-mixing stopped-flow experiment measuring a rate constant for the proton dissociation from reduced P2O. A solution of reduced P2O ( $96 \mu\text{M}$  before mixing) in 5 mM MES and 100 mM sodium sulfate, pH 5.5 was mixed with 100 mM of anaerobic CHES buffer, pH 9.0 in the first mixing step with age times of 40 ms, 60 ms, 90 ms and 1 s. The resulting solutions were then mixed with 100 mM CHES pH 9.0 containing 0.96 mM oxygen in the second mixing. The final solution contained the reduced enzyme of  $24 \mu\text{M}$  and oxygen of 0.48 mM in buffer at pH 9.0 and the experiment was done at  $4^\circ\text{C}$ . (A) Kinetic traces monitored at the 395 nm indicated that the amplitude of absorbance at 395 nm after the first phase decreased when the age time was increased. The inset shows a plot of the amplitudes of the first phase versus the age time. (B) Kinetic traces monitored at 458 nm indicated that upon increasing the age time, the oxidation kinetics was slower (the trace shifted from the left to the right).



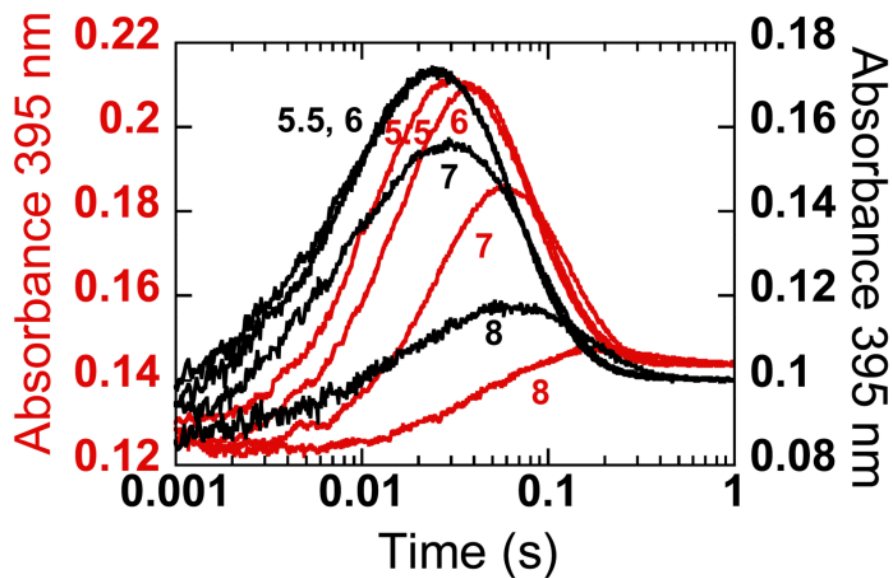
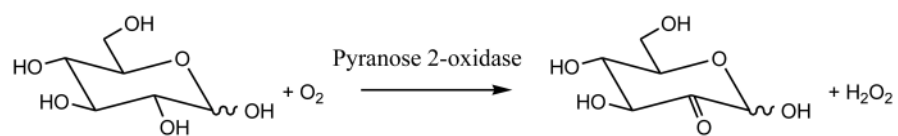
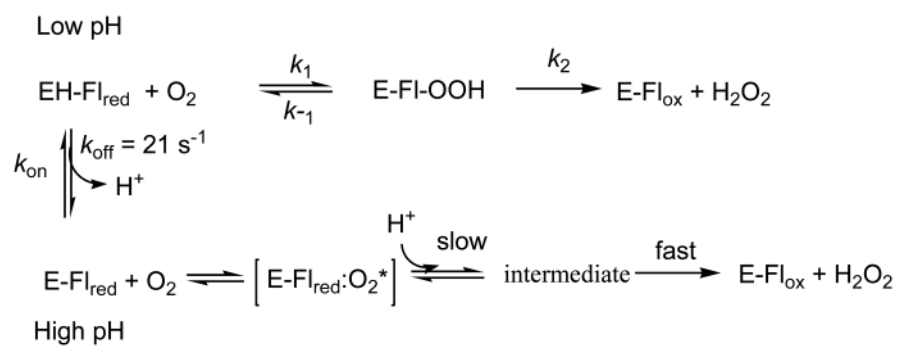


**Figure 6.**

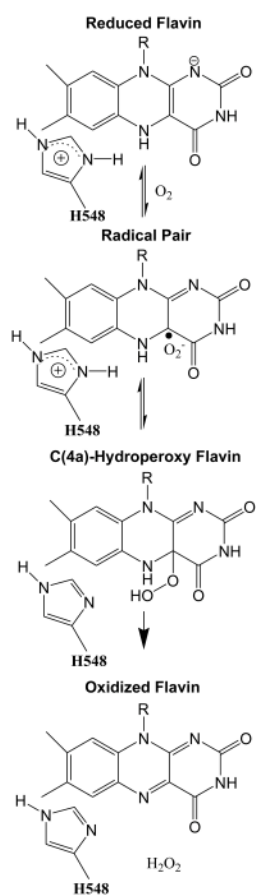
Oxidations of reduced P2O performed by pH-jump mixing from pH 9.0 to various pH values. A solution of 58  $\mu\text{M}$  reduced P2O in 5 mM CHES containing 100 mM sodium sulfate pH 9.0 was mixed with 100 mM buffers pH 5.5, 6.0, 7.0, 8.0 at 4  $^{\circ}\text{C}$ . Final solutions contained the reduced P2O of 29  $\mu\text{M}$  and oxygen concentration of 0.96 mM oxygen. The kinetic traces of the reactions monitored at 395nm were plotted on the left Y-axis (red traces). Kinetic traces from figure 1 data (20  $\mu\text{M}$  P2O) at the same pH (black traces) were overlaid for comparison.



**Scheme 1.**  
Reaction of pyranose 2-oxidase.



**Scheme 2.**  
Reaction Mechanism of the oxidative half-reaction of pyranose 2-oxidase at low and high pH.

**Scheme 3.**

**Table 1**

Effects of pH on kinetic parameters of the oxidative half-reaction of P2O.

pH	$k_{app}$ of the first phase ( $M^{-1}s^{-1}$ )	$k_{app}$ of the second phase( $s^{-1}$ )
5.5	$7.5 \pm 0.8 \times 10^4$	$28 \pm 5$
6.0	$7 \pm 1 \times 10^4$	$29 \pm 5$
6.5	$6.8 \pm 0.4 \times 10^4$	$30 \pm 6$
7.0 <sup>a</sup>	$5.6 \pm 0.2 \times 10^4$	$24 \pm 2$
7.5	$6.7 \pm 0.5 \times 10^4$	$21 \pm 2$
8.0	$2.3 \pm 0.8 \times 10^4$	$11.6 \pm 0.1$
8.5	-	$4.1 \pm 0.2$
9.0	-	$3.4 \pm 0.1$
9.5	-	$2.1 \pm 0.1$
10.0	-	$1.3 \pm 0.3$

<sup>a</sup>(Sucharitakul 2011)